

See discussions, stats, and author profiles for this publication at: <https://www.researchgate.net/publication/321433141>

Lateral-Load Resistance of Cross-Laminated Timber Shear Walls

Article in *Journal of Structural Engineering* · December 2017

DOI: 10.1061/(ASCE)ST.1943-541X.0001912

CITATIONS

6

READS

336

6 authors, including:



Thomas Reynolds

The University of Edinburgh

29 PUBLICATIONS 173 CITATIONS

SEE PROFILE



Robert Foster

University of Cambridge

18 PUBLICATIONS 49 CITATIONS

SEE PROFILE



Julie Bregulla

Building Research Establishment BRE

16 PUBLICATIONS 107 CITATIONS

SEE PROFILE



Wen-Shao Chang

The University of Sheffield

88 PUBLICATIONS 320 CITATIONS

SEE PROFILE

Some of the authors of this publication are also working on these related projects:



Dynamic performance of UK domestic timber floors [View project](#)



Glued-in rods for timber structures [View project](#)

LATERAL LOAD RESISTANCE OF CROSS-LAMINATED TIMBER SHEAR WALLS

Thomas Reynolds Ph.D. C.Eng¹

Robert Foster Ph.D.²

Julie Bregulla Ph.D. C.Eng³

Wen-Shao Chang Ph.D.⁴

Richard Harris C.Eng⁵

Michael Ramage Ph.D. C.Eng⁶

This is the author's accepted version, the published version in the ASCE Journal of Structural Engineering is at [http://dx.doi.org/10.1061/\(ASCE\)ST.1943-541X.0001912](http://dx.doi.org/10.1061/(ASCE)ST.1943-541X.0001912). Please cite as: J. Struct. Eng., 2017, 143(12): 06017006

ABSTRACT

Cross-laminated timber shear wall systems are used as a lateral load resisting system in multi-story timber buildings. Walls at each level typically bear directly on the floor panels below and are connected by nailed steel brackets. Design guidance for lateral load resistance of such systems is not well established and design approaches vary among practitioners. Two cross-laminated two-story timber shear wall systems are tested under vertical and lateral load, along with pull-out tests on individual steel connectors. Comprehensive kinematic behavior is obtained from a combination of discrete transducers and continuous field displacements along the base of the walls, obtained by digital image correlation, giving a measure of the length of wall in contact with the floor below. Existing design approaches are evaluated. A new offset-yield criterion based on acceptable permanent deformations is proposed. A lower bound plastic distribution of stresses, reflecting yielding of all connectors in tension and cross-grain crushing of the floor panel, is found to most accurately reflect the observed behavior.

BACKGROUND

Cross-laminated timber (CLT) is a panelised glued-laminated mass timber structural product, comprising sawn timber sections, laid-up in layers, with each layer at right angles to the adjacent layer. CLT floor and wall elements have consequently been used to form the principal vertical and lateral load resisting systems of multi-story buildings around the world. A number of benefits have been attributed to CLT in mid-rise construction including: low dust, low noise, light craneage, high tolerances, reduced onsite waste, reduced construction times, low number of person-hours on site

¹Chancellor's Fellow, School of Engineering, University of Edinburgh, Edinburgh EH9 3JL, UK Email: t.reynolds@ed.ac.uk

²Senior Lecturer, School of Civil Engineering, The University of Queensland, Brisbane St Lucia, QLD 4072, Australia

³Director, Building Technology Group, BRE, Bucknalls Lane, Watford WD25 9XX

⁴Lecturer, BRE Centre for Innovative Construction Materials, University of Bath, Claverton Down, Bath BA2 7AY

⁵Honorary Professor, BRE Centre for Innovative Construction Materials, University of Bath, Claverton Down, Bath BA2 7AY

⁶Senior Lecturer, University of Cambridge, Department of Architecture, 1 Scroope Terrace, Cambridge CB2 1PX

and negative embodied carbon (if carbon sequestration of forests is taken into account) (Waugh et al. 2009; FII and BSLC 2014).

A common CLT construction method that can offer considerable advantages for builders is that of platform construction, whereby the CLT floor slab bears directly on the CLT walls below. Each story then forms a stable working platform onto which the story above is built. Forces in the wall elements must therefore pass through the floor plate in the much weaker, less stiff, cross-grain direction.

Literature Review

In CLT construction in non-seismic zones, evenly spaced angle brackets connect perpendicular panels at vertical intersections between walls and at horizontal wall-floor intersections. In seismic applications, taller hold-down brackets are provided at either end of the panel to resist uplift, while the shorter angle brackets are assumed purely to resist shear. This configuration of connectors is the subject of much experimental investigation into the lateral load resistance of single-storey CLT shear wall systems (Ceccotti et al. 2010; Pei et al. 2012; Schneider et al. 2012; Pei et al. 2013; Shen et al. 2013; Flatscher et al. 2015; Gavric et al. 2015; Li and Lam 2015; Popovski and Gavric 2016; Tomasi and Smith 2015; Casagrande et al. 2016). Numerical models are proposed which replicate the hysteretic response of timber shear wall systems (Shen et al. 2013; Li and Lam 2015; Pozza et al. 2014). These models assume that the movement of each panel comprises rotation about the corner and horizontal sliding, an approach which represents a simplification of earlier models used for sheathed timber-frame walls (Dolan and Foschi 1991; Folz and Filiatrault 2001), since the in-plane deformation of the CLT panel itself is taken to be sufficiently small to assume quasi-rigid behavior.

While the assumption of rotation around the corner of the panel is shown to give an accurate estimate of the measured push-over response (Pei et al. 2012; Pei et al. 2013; Shen et al. 2013; Casagrande et al. 2016), it is theoretically unconservative because it assumes that an infinite stress can be tolerated at the corner. In reality, the compressive force due to overturning must be transferred over a suitable bearing length at the compression end of the wall.

Practicing engineers from two companies active in CLT design described the methods they use to estimate lateral load resistance. One engineer noted that different models are adopted in different circumstances, with modified elastic-plastic methods being preferred in all but the most onerous design cases. Another noted that there has been a progression in recent years from predominantly elastic design, to elastic-plastic models influenced by observed behavior of panels. The additional need to verify the buckling capacity of the compressive end of the wall was highlighted by consultants at both firms. All engineers noted the lack of standardized guidance for the design of CLT shear walls. The Canadian Edition of the CLT Handbook SP528E (Gagnon and Pirvu 2011) observes candidly that, ‘Not much information is available in the literature for CLT walls subjected to in-plane loading’. There is published guidance outside of standards in the US (Karakabeyli and Douglas 2013) and the UK (TRADA 2009; TRADA 2014), as well as in the academic studies described above, and these have been used in choosing the design methods tested in this study.

In this study, novel lateral load tests were used to obtain a comprehensive measurement of the kinematics of a two-storey CLT platform shear wall system subject to combined vertical and lateral load, with and without a vertical half lap joint and return wall. The objective was to compare a number of design methods based on force equilibrium at the base of the wall, and assess their

accuracy for this particular case.

MATERIALS AND METHODS

General layout and materials

The thickness and build-up of laminates in the CLT panels were the same in all tests, including individual connections and complete shear walls: an 85 mm thick panel built up of five 17 mm layers. The panels were supplied by Metsä wood (Espoo, Finland) as being from C24 Spruce according to European Norm EN338 (2009). Moisture content was measured immediately after testing by the electrical resistance method, and was 10.5% (coefficient of variation (COV) 0.07) for the connection tests, and 8.0% for the panel tests (COV 0.07). The mean density of the CLT panels, adjusted for 12% moisture content, was 444 kg m^{-3} (COV 0.02).

Angle-bracket connections (Simpson Strong Tie ®ABR-100, Tamworth, UK) nailed to CLT elements were tested, using proprietary angle brackets and ring-shank nails. A vertical CLT element 460 mm by 200 mm was connected by a single bracket to a horizontal element 770 mm by 200 mm. Rotation of the upper piece was prevented by a prop with a roller bearing.

The properties of the angle brackets are given in European Technical Approval ETA-06/0106 (2013). The brackets were fully nailed with 4.0×60 ring-shank nails, with 4 mm diameter and 60 mm length, 10 to the vertical leg and 14 to the horizontal leg. 12 connections were tested according to BS EN 26891 (1991). The specimens were also used for a separate study investigating behavior in the serviceability limit state. Before monotonic loading to failure, therefore, they were subjected to 1000 fully-reversed cyclic loads with peak values of 20% and 40% of their characteristic resistance according to ETA-06/0106 (2013).

Two-storey high specimens were tested, giving a more realistic ratio of shear to overturning moment on the panels than for a single-story specimen, and allowing for a ‘floor’ panel between the walls and at the base. Fig. 1 illustrates the test setup and key dimensions. The precise position of the tension bars along the 2 m length of the wall was determined by the location of the anchor points in the strong floor, and is shown in Fig. 1. The measured centroid of the vertical force along the length of the wall was used in the calculations in Table 1.

Angle brackets were spaced at 400 mm centers, starting 100 mm from one edge of the wall. Brackets on either side of the wall were staggered by 200 mm. The screwed half lap joint was formed using Simpson Strong Tie®Eurotec 8.0×80 screws, with an inner thread diameter of 6 mm, an outer thread diameter of 8 mm and a length of 80 mm. The screws were spaced at 100 mm, starting 50 mm from the panel edge. The half lap joint was 50 mm wide.

A constant vertical load was applied, spread by a steel channel section across the length of the wall to avoid concentrated force under the two points of application. A load of 32 kN was used, to represent four lightweight story loads of 4 kN m^{-2} , with a 4 m width spanning onto the wall. Steel bars in tension applied the vertical load to the wall in both tests. The load was kept constant by an operator continually adjusting the hydraulic jacks at the base of these bars according to the force measured there.

The complete shear walls were tested initially in repetitive load cycles, with a maximum lateral force of 10 kN, after which the displacement was increased at approximately 5 mm/min. The loading pattern aligned with the intent of BS EN 594 (2011), which provides a method to measure lateral stiffness and strength of shear walls.

Digital image correlation was used to make spatially continuous measurement of displacement along the lower edge of the bottom panel of the shear wall specimen. A line approximately 150 mm

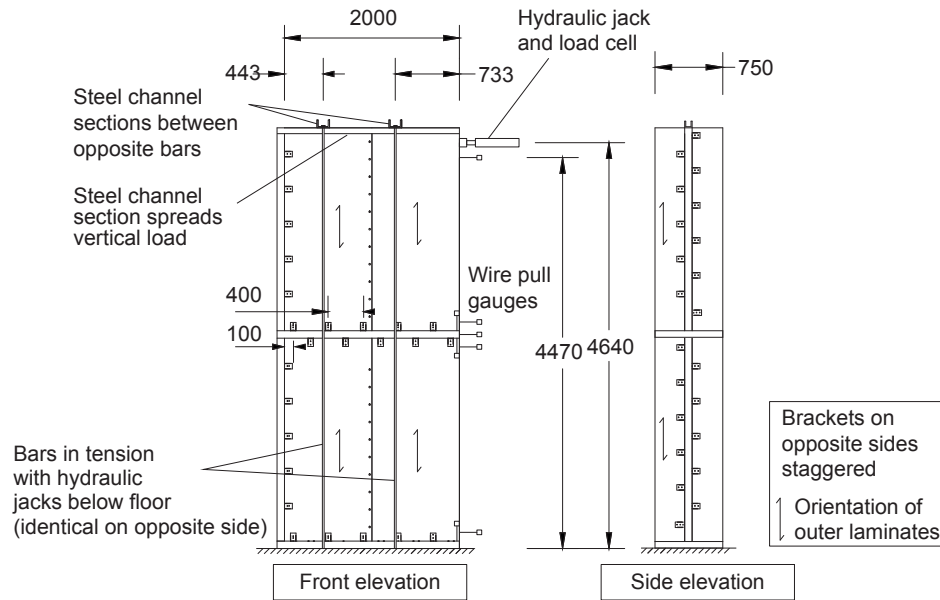


FIG. 1. Test setup and dimensions for shear-wall tests - the specimen with half lap joint is shown (dimensions in mm)

above the base of the wall was tracked, above the angle brackets, since their reflective surface was not suitable for digital image correlation. A pattern recognition grid with 50 mm by 50 mm interrogation cells was used.

RESULTS

Predicted behavior

The resistance to the overturning moment was calculated as the force couple between the bearing of the wall panel on the floor and the hold-down force from the connections. Each method assessed the capacity of the angle brackets to resist uplift and sliding, and the timber in the floor to resist compression. Since there is limited empirical data for combined loading on brackets, each bracket was taken to resist either uplift or sliding. The connection tests gave a peak resistance to uplift ranging from 12.0 kN to 17.6 kN, with a mean of 14.9 kN, and an estimated 5th percentile of 12.1 kN, and the resistance to sliding was taken from ETA-06/0106 (2013). Serrano and Enquist (2010) measured a mean compression strength, defined by a 1% strain offset, of 5.8 MPa for this orientation, for CLT with density 427 kg m^{-3} at 10% moisture content, and this compression strength is used to estimate the strength in bearing of the CLT in these tests.

Each method is illustrated in Fig. 2. Seismic calculations in the literature (Pei et al. 2012; Pei et al. 2013; Shen et al. 2013; Casagrande et al. 2016) include a non-linear characterization of the force-displacement response of each connection. Since this information is unlikely to be available to a practising engineer for each type of connection, the methods here assume either an elastic variation of force in the connections, or that they have reached their yield force.

The first method considered the overturning moment in isolation, with a zone of one third of the wall width in compression, and the connections within the opposite third of the wall width

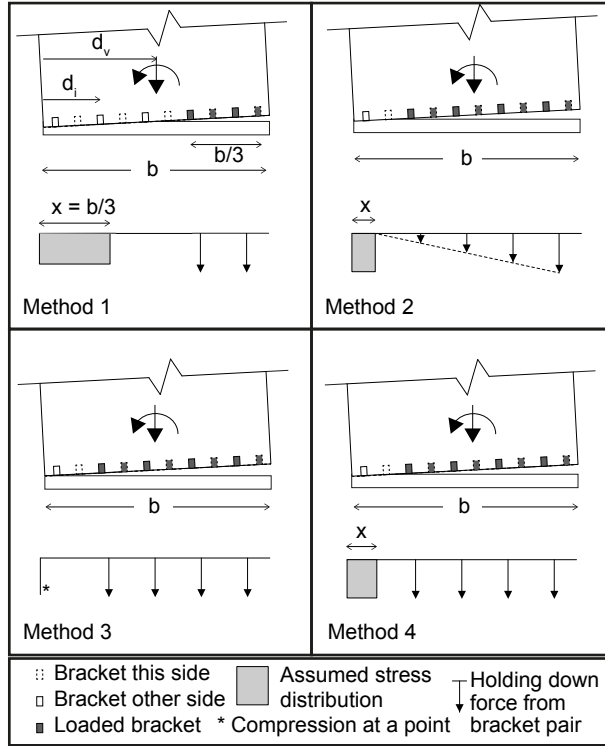


FIG. 2. Assumed simplified force balance at base of wall for each case - all connections are assumed to be at their full capacity

activated to resist uplift. Method 2 used an elastic variation of stress in the connectors, including the effect of the vertical load, as proposed in principle in the US Edition of the CLT Handbook SP-529-E (Karakabeyli and Douglas 2013) for wind loading. Method 3 assumed the wall to pivot around a point, as in the calculation of the required hold-down forces in the TRADA guidance and worked example (TRADA 2009; TRADA 2014). Method 4 assumed a length of wall in uniform compression so that the compressive stress was equal to the strength of the floor panel, with this length determined by equilibrium with the forces in the connections and the forces applied to the shear wall. In each case, the length of the wall in compression was assumed to be in a fully-plastic state, with the whole length at a stress equal to its full strength.

The overturning resistance M_u for the shear wall system based on methods 1, 3 and 4 is given by Equation (1), while method 2 varies the force in the connectors according to their distance from the compression zone edge, as in Equation (2). F_u is the capacity of the connections, d_i is the distance of connector i from the compression edge, x is the length of the compression zone, V is the vertical load applied to the wall, at d_v from the compression edge.

$$M_{u,1,3,4} = \sum_i F_u \left(d_i - \frac{x}{2} \right) + V \left(d_v - \frac{x}{2} \right) \quad (1)$$

$$M_{u,2} = \sum_i \left[F_u \frac{d_i - x}{\max_i (d_i - x)} \right] \left(d_i - \frac{x}{2} \right) + V \left(d_v - \frac{x}{2} \right) \quad (2)$$

TABLE 1. Dimensions for force balance according to each design method

Method	Compression Zone (x)	Connectors Resisting Uplift (i)
1	$\frac{b}{3}$	$\frac{2b}{3} < d_i < b$
2	to limit σ_c *	$d_i > x$ †
3	0	$d_i > x$ †
4	to limit σ_c *	$d_i > x$ †

* x chosen so that σ_c is set to its limiting value

† any connectors required to resist sliding are excluded

Symbols used are as in Equations (1) to (5) and Fig. 2

The sliding resistance of the wall system S_u is given by Equation (3), where F_s is the sliding resistance of the connector. Connectors i are assumed to resist only uplift, and connectors j are assumed to resist only sliding, thus avoiding the design of connectors for combined uplift and sliding, for which there is limited experimental data and no current design guidance. μ is the coefficient of friction assumed for the interface between wall and floor, taken to be 0.2 in this case.

$$S_{u,1,3,4} = \sum_j F_s + \mu \left(\sum_i F_u + V \right) \quad (3)$$

The compressive stress was calculated by Equation (4) for methods 1, 3 and 4, and by Equation (5) for method 2. Table 1 shows how the compression zone x and the connectors i contributing to uplift resistance are chosen in each method. w is the width of the wall.

$$\sigma_c = \frac{V + \sum_i F_u}{xw} \quad (4)$$

$$\sigma_c = \frac{V + \sum_i F_u \frac{d_i - x}{\max_i(d_i - x)}}{xw} \quad (5)$$

Shear-wall tests

The results of the tests on both shear wall systems are shown in Fig. 3. The initial stiffness was higher for the jointed panel with return wall. Both tests were stopped because excessive deflection at the loading point meant that the loading jack would have lost contact with the load cell attached to the panel, and at this point, both tests had reached a load approximately equal to the load predicted by method 3, and in the jointed panel with return wall a similar load was predicted by method 4. The load cell used to measure the applied lateral force was seen to be damaged due to off-centre loading near the end of the single panel test, at approximately 80 mm displacement, and was replaced. This was not, however, considered to affect the load measurements shown in Fig. 3 before that displacement, and so does not affect the conclusions in this study. Measurements after the point of damage are shown in grey.

An alternative measure of the strength of the wall system is the offset yield point used, for example, to describe timber connections (ASTM 2002). An offset equal to the height of the displacement measurement divided by 300, or 14.9mm, was used to correspond to a residual

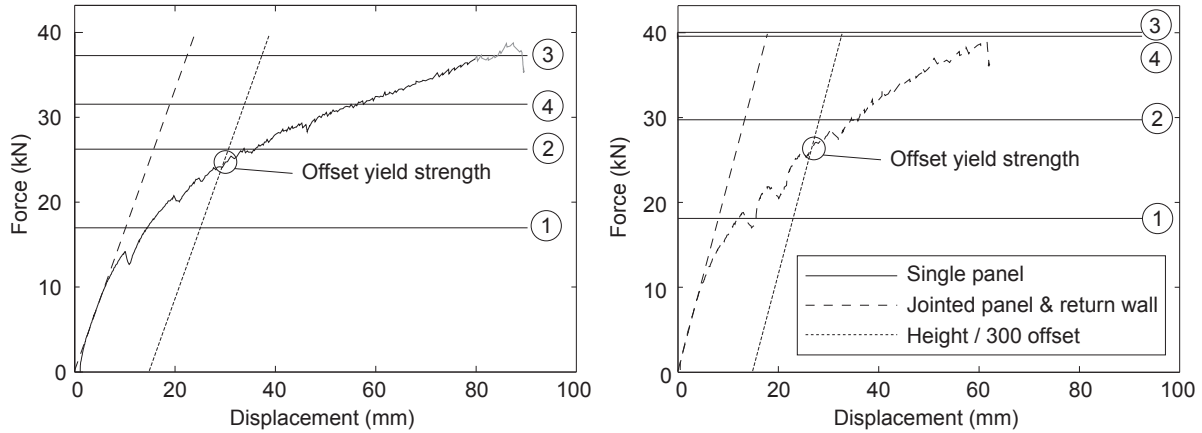


FIG. 3. Force-displacement diagrams for the static lateral load tests on the shear wall system for the full-panel specimen, and for the jointed panel specimen with return wall - the numbered lines 1 to 4 represent the predicted peak load according to the four methods

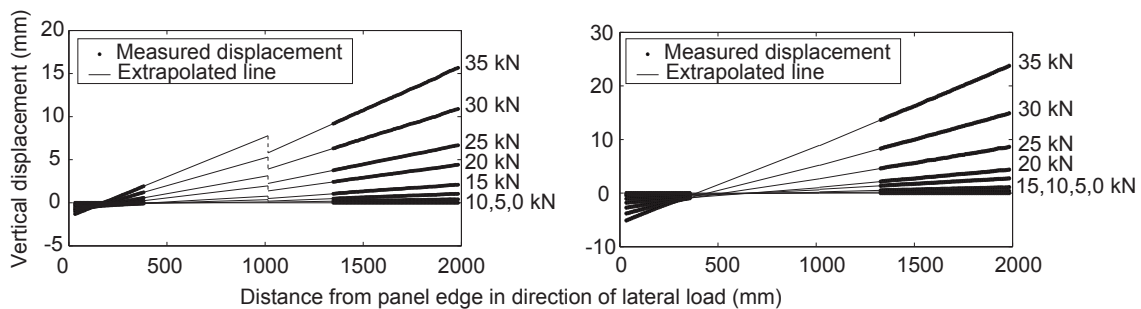


FIG. 4. Vertical displacement along the lower edge of the lower panel of the shear wall for each specimen, in 5 kN increments of lateral load up to 35 kN - the extrapolated lines cover the area obstructed in the digital images

displacement in the range of permitted drift for serviceability of multi-story buildings (BSI 2005). This ‘offset strength’ is 24.1 kN for the panel without return wall, and 25.6 kN for the panel with half lap and return wall. These values may be considered more useful for design than the maximum load, since they do not rely on the substantial secondary ‘hardening’ behavior observed after a reduction from the initial elastic stiffness. This offset yield point falls close to the elastic limit calculated by method 2.

Digital image correlation showed the movement of the lower wall panel in both the ultimate load tests. It tracked the movement of the lower edge of the panel through a series of images taken at steps of 5 kN in the lateral load, shown in Fig. 4 for each specimen.

The position of the contact zone edge moves towards the compression edge as the load is increased. The location of the contact zone edge for the single-panel test ranges from 0.77 m from the edge of the panel at 5 kN lateral force, to 0.34 m at 35 kN. The contact zone edge in the shear wall with both the half lap and return wall is closer to the compression edge of the wall, ranging

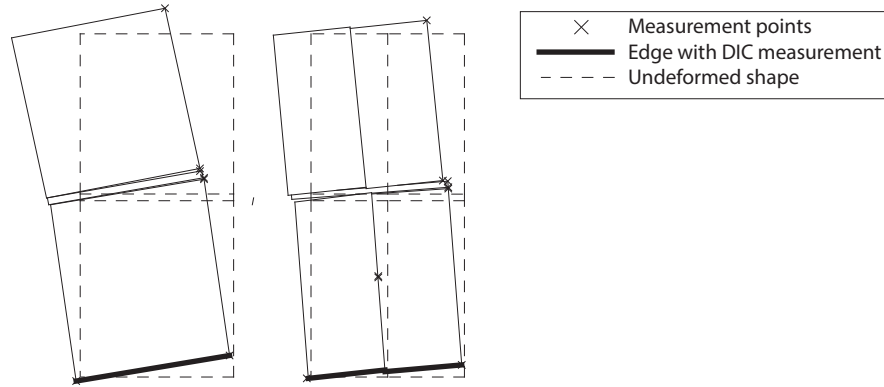


FIG. 5. The deformed shape for an applied lateral load of 35 kN, exaggerated by a factor of ten - the exaggeration of the displacement leads to slight distortion of the panels

from 0.46 m at 5 kN to 0.16 m at 35 kN. Irreversible embedment in this area will contribute to the residual displacements observed after unloading in both tests - there was a residual horizontal displacement at the top of the wall of 36.3 mm for the single panel and 21.5 mm for the panel with the half lap connection.

By combining the displacements measured by digital image correlation with those measured by the linear displacement transducers, a deformed shape was calculated and is shown in Fig. 5. Displacements at points which were not measured were calculated assuming rigid body rotation and translation of each panel in plane, an assumption justified by the results of the digital image correlation measurements along the base of the panel. The image shows that the central floor panel in the system with the half lap joint has flexed and crushed out of plane to fit with the rotation of the four wall panels.

DISCUSSION

These tests built up a full picture of how the shear wall system moves under load to feed into an assessment of how it resists the loads applied to it. Method 3, which assumes the lower wall to pivot around its extreme edge, gives a predicted load capacity closest to the peak loads measured, and for the test with the return wall, the predicted load exceeded the peak observed load by approximately 3%. The measurements of the length of the contact zone in compression at the base of the lower wall, however, correlate well with force distribution method 4, so it is not readily clear why the predicted load based on method 4 was exceeded by approximately 20% in the single panel tests. A possible explanation for a discrepancy between the tests on individual connections and the single panel tests was the different cyclic loads applied to them: more cycles, at a higher percentage of the eventual failure load, were applied to the connectors, and this may have reduced the maximum load resistance in the connection tests. It is considered that the residual stiffness in the nails could be sufficient to explain the continued increase in load at the end of the test, and it therefore appears that the maximum load for each of the specimens was not reached.

CONCLUSION

This study has brought out new knowledge of the deformation and load resistance of a common structural system using CLT: that of platform construction. The measured deformations of the

two-storey shear wall systems showed that, under ultimate loading, the movement of the complete shear wall was dominated by rigid-body movement of the panels, and that the screwed half lap joint was effective in allowing the two panels to act compositely.

Some of the simple design calculation methods currently used by structural engineers substantially underestimated the peak load resistance of this system. The most accurate design method for the maximum load resisted by this wall system assumes the panel to rotate about the compression edge of the wall (Method 3). However, this method requires the unrealistic assumption that the compression is transferred at a point.

The measured length of contact along the base of the wall tended towards that predicted by an equilibrium condition with a fully plastic zone in the timber loaded perpendicular to grain, and fully plastic forces in all connections (Method 4).

Method 4 is, therefore, considered to best capture the system behavior near the maximum resistance, however the maximum resistance in these tests was associated with excessive deformations. For this reason an offset yield criterion for design was proposed. Method 2, based on equilibrium of a rectangular compression stress block and linear elastic distribution of connector forces, limited by yield of the first exterior connector at the base of the wall, lay close to this offset yield strength for this system.

ACKNOWLEDGMENTS

The authors express their gratitude to Chris Yapp and the other technicians at the BRE Structures Laboratory for their contribution to the experimental design and carrying out the tests. The experimental part of this work was funded by a BRE Trust grant, and the investigation of design methods was carried out under a Leverhulme Trust Programme Grant and EPSRC grant EP/M01679X/1. The authors are also grateful to Simpson Strong Tie® for providing angle brackets and nails free of charge.

REFERENCES

- ASTM (2002). “ASTM D5764 Standard Test Method for Evaluating Dowel-Bearing Strength of Wood and Wood-.” , ASTM.
- BSI (1991). “BS EN 26891:1991 Timber structures. Joints made with mechanical fasteners. General principles for the determination of strength and deformation characteristics.” , BSI.
- BSI (2005). “NA to BS EN 1993-1-1 UK National Annex to Eurocode 3: Design of steel structures Part 1-1: General rules and rules for buildings.” , BSI.
- BSI (2009). “BS EN 338: 2009 Structural timber. Strength classes.” , BSI.
- BSI (2011). “BS EN 594:2011 Timber structures. Test methods. Racking strength and stiffness of timber frame wall panels.” , BSI.
- Casagrande, D., Rossi, S., Sartori, T., and Tomasi, R. (2016). “Proposal of an analytical procedure and a simplified numerical model for elastic response of single-storey timber shear-walls.” *Construction and Building Materials*, 102, 1101–1112.
- Ceccotti, A., Sandhaas, C., and Yasumura, M. (2010). “Seismic Behaviour of Multistory Cross-laminated Timber Buildings.” *International Convention of Society of Wood Science and Technology and United Nations Economic Commission for Europe Timber Committee*, United Nations, Geneva, Switzerland (October).
- Dolan, J. D. and Foschi, R. O. (1991). “Structural Analysis Model for Static Loads on Timber Shear Walls.” *Journal of Structural Engineering*, 117(3), 851–861.

- EOTA (2013). “European technical approval eta-06/0106.” , European Organisation for Technical Approvals.
- FII and BSLC (2014). “Summary report: Survey of international tall wood buildings.” , Forestry Innovation Investment, Vancouver, BC, and BSLC, Surrey, BC.
- Flatscher, G., Bratulic, K., and Schickhofer, G. (2015). “Experimental tests on cross-laminated timber joints and walls.” *Proceedings of the Institution of Civil Engineers - Structures and Buildings*, 168(11), 868–877.
- Folz, B. and Filiatrault, A. (2001). “Cyclic Analysis of Wood Shear Walls.” *Journal of structural engineering*, 127(4), 433–441.
- Gagnon, S. and Pirvu, C. (2011). “CLT Handbook: Canadian Edition, Special Publication SP-528E.” , FPIInnovations, Quebec City, Canada.
- Gavric, I., Fragiaco, M., and Ceccotti, A. (2015). “Cyclic behaviour of typical metal connectors for cross-laminated (CLT) structures.” *Materials and Structures*, 48(6), 1841–1857.
- Karakabeyli, E. and Douglas, B. (2013). *CLT Handbook*. FPIInnovations, us edition edition.
- Li, M. and Lam, F. (2015). “Lateral Behaviour of Cross Laminated Timber Shear Walls under Reversed Cyclic Loads.” *Proceedings of the Tenth Pacific Conference on Earthquake Engineering*, Seismology Research Centre, Victoria, Australia .
- Pei, S., Lindt, J. V. D., and Popovski, M. (2013). “Approximate R-Factor for Cross Laminated Timber Walls in Multi-Story Buildings.” *Journal of Architectural . . .* , 19(December), 245–255.
- Pei, S., Popovski, M., and Van de Lindt, J. W. (2013). “Analytical study on seismic force modification factors for cross-laminated timber buildings.” *Canadian Journal of Civil Engineering*, 40(9), 887–896.
- Popovski, M. and Gavric, I. (2016). “Performance of a 2-Story CLT House Subjected to Lateral Loads.” *Journal of Structural Engineering*, 142, E4015006.
- Pozza, L., Scotta, R., Trutalli, D., Pinna, M., Polastri, A., and Bertoni, P. (2014). “Experimental and Numerical Analyses of New Massive Wooden Shear-Wall Systems.” *Buildings*, 4(3), 355–374.
- Schneider, J., Stiemer, S. F., Tesfamariam, S., Karacabeyli, E., and Popovski, M. (2012). “Damage assessment of cross laminated timber connections subjected to simulated earthquake loads.” *World Conference on Timber Engineering*, New Zealand Timber Design Society, Auckland, New Zealand, 398–406.
- Serrano, E. and Enquist, B. (2010). “Compression Strength Perpendicular to Grain in Cross-Laminated Timber (CLT).” *World Conference on Timber Engineering*, CNR IVALSA, Italy.
- Shen, Y.-L., Schneider, J., Tesfamariam, S., Stiemer, S. F., and Mu, Z.-G. (2013). “Hysteresis behavior of bracket connection in cross-laminated-timber shear walls.” *Construction and Building Materials*, 48, 980–991.
- Tomasi, R. and Smith, I. (2015). “Experimental Characterization of Monotonic and Cyclic Loading Responses of CLT Panel-To-Foundation Angle Bracket Connections.” *Journal of Materials in Civil Engineering*, 27(6), 04014189.
- TRADA (2009). “Guidance Document 10 (GD10) Cross-laminated Timber (Eurocode 5) Design Guide for Project Feasibility.” , TRADA Technology.
- TRADA (2014). “Worked Example: 12-storey building of cross-laminated timber.” , TRADA Technology.
- A. Waugh, K. H. Weiss, and M. Wells, eds. (2009). *A Process Revealed - Auf Dem Holzweg*. FUEL, London.